



*Supplement of*

## **Linking heavy rainfall to suspended sediment fluxes in a deglaciating Alpine catchment**

**Amalie Skålevåg et al.**

*Correspondence to:* Amalie Skålevåg ([skalevag2@uni-potsdam.de](mailto:skalevag2@uni-potsdam.de))

The copyright of individual parts of the supplement might differ from the article licence.

## Contents

	<b>S1 Study area, data and methods</b>	<b>2</b>
	S1.1 Land cover within study area . . . . .	2
	S1.2 Weather stations . . . . .	3
5	S1.3 IDF curves . . . . .	5
	<b>S2 Additional results and figures</b>	<b>6</b>
	S2.1 INCA uncertainty . . . . .	6
	S2.2 Heavy precipitation events and characteristics . . . . .	8
	S2.2.1 Events removed due to unrealistic precipitation . . . . .	8
10	S2.2.2 Trend in numbers of heavy precipitation events . . . . .	8
	S2.3 Precipitation characteristics and sediment response . . . . .	11
	S2.3.1 Sediment response of heavy precipitation by spatial scale . . . . .	11
	S2.4 Choice of linear regression model . . . . .	11
	S2.4.1 Distribution of bootstrapped slopes . . . . .	14
15	S2.5 All event metrics by temporal scale . . . . .	15

## S1 Study area, data and methods

### S1.1 Land cover within study area

#### CORINE Land Cover 2018

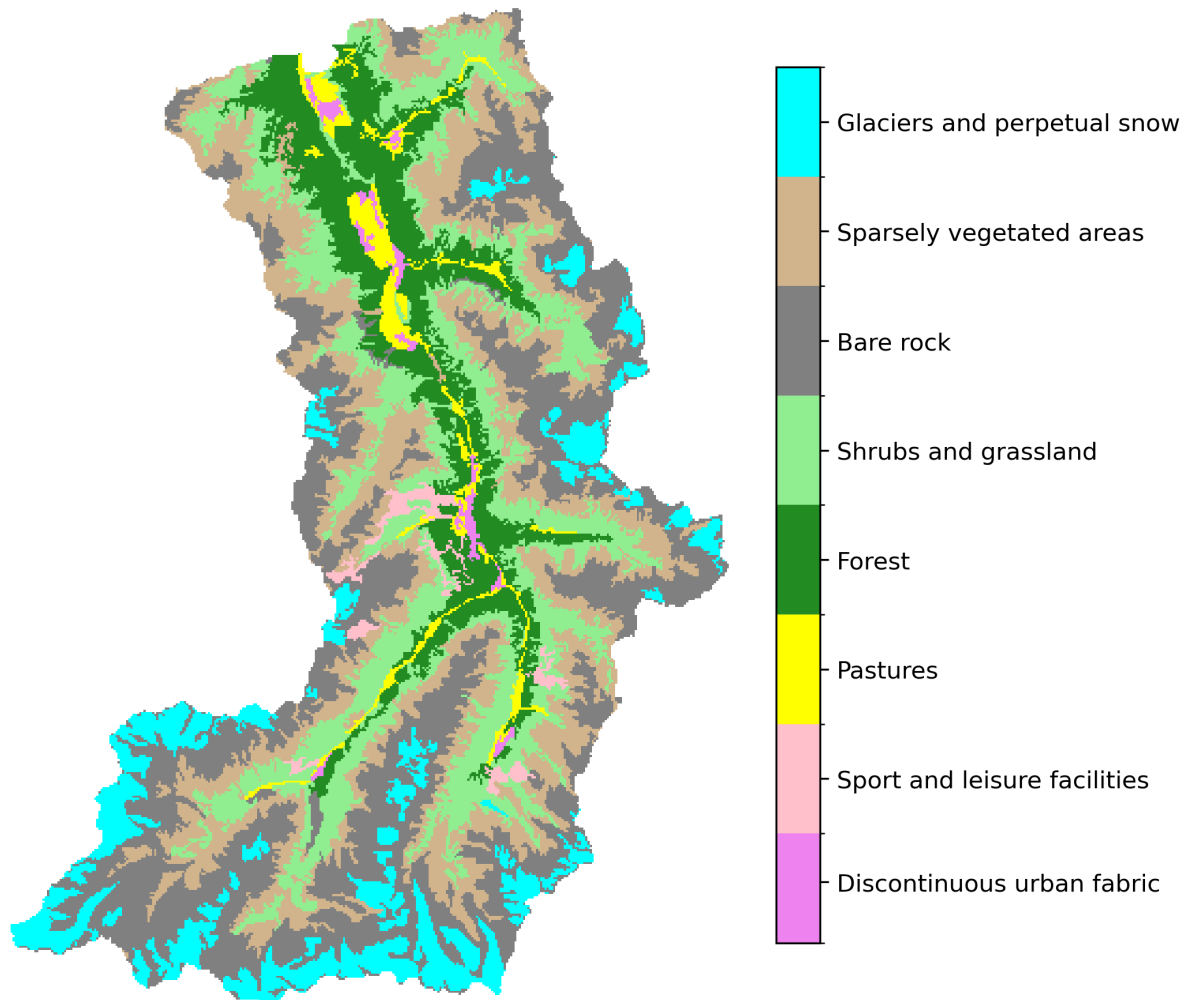


**Figure S1.** Land cover in Tumpen-Ötztal as mapped in CORINE Land Cover 2018 (Copernicus Land Monitoring Service, 2020).

## S1.2 Weather stations

**Table S1.** Weather stations in and around Ötztal with precipitation observations used to evaluate the uncertainty of INCA gridded precipitation. Most stations are operated by GeoSphere Austria (GSA) or the Hydrographic Service of Tyrol (HD-Tirol) with additional stations operated by the Department of Geography (UIBK-GEOG) and the Department of Atmospheric and Cryospheric Sciences (ACINN) at the University of Innsbruck, and the Bavarian Academy of Sciences (BADW). The original data had temporal resolutions ranging from 1-min to daily and has varying temporal extents. For an overview of available data during the study period see Fig. S2.

Name	Station	Location			Temporal	
	Operator	Latitude	Longitude	Altitude	Resolution	Extent
Stams	HD-Tirol	47.2744	10.98528	711	daily	1971-2021
Oetz	HD-Tirol	47.2058	10.88611	760	daily	1971-2021
Imst-Oberstadt	HD-Tirol	47.2489	10.74111	860	daily	1971-2021
Ried-im-Oberinntal	HD-Tirol	47.0575	10.66056	895	daily	1971-2021
Jerzens-Ritzenried	HD-Tirol	47.1225	10.78194	1120	daily	1971-2021
Längenfeld <sup>a</sup>	HD-Tirol	47.0763	10.97000	1180	daily	1971-2021
Gries-im-Sellrain	HD-Tirol	47.1886	11.15250	1227	daily	1971-2021
Kaunertal-Vergötschen	HD-Tirol	47.0431	10.75306	1269	daily	1971-2021
St.Leonhard-i.P.	HD-Tirol	47.0761	10.83889	1329	daily	1971-2021
Sölden <sup>a</sup>	HD-Tirol	46.9850	11.01472	1332	daily	1971-2021
Ladis-Neuegg	HD-Tirol	47.0972	10.64889	1426	daily	1971-2021
Gries <sup>a</sup>	HD-Tirol	47.0700	11.02667	1590	daily	1998-2021
Plangeröß	HD-Tirol	46.9875	10.86750	1605	daily	1971-2021
Ochsen Garten-Obergut	HD-Tirol	47.2300	10.91861	1695	daily	1971-2021
Hintere-Fundusalm <sup>a</sup>	HD-Tirol	47.1028	10.88611	1960	15-min	2020-2023
Dresdner-Hütte	HD-Tirol	46.9975	11.14000	2290	daily	1979-2021
Innsbruck-Flugplatz	GSA	47.2600	11.35667	578	hourly	1992-2024
Innsbruck-Univ-	GSA	47.2600	11.38417	578	hourly	1986-2024
Haiming	GSA	47.2597	10.88944	659	hourly	2007-2024
Imst	GSA	47.2369	10.74222	773	hourly	2007-2024
Landeck	GSA	47.1403	10.56361	796	hourly	1993-2024
Neustift-Milders	GSA	47.1028	11.29195	1007	hourly	2004-2024
Umhausen <sup>a</sup>	GSA	47.1392	10.92889	1035	hourly	2003-2024
St-Leonhard-Pitztal	GSA	47.0272	10.86556	1454	hourly	2007-2024
Obergurgl <sup>a</sup>	GSA	46.8670	11.02445	1941	hourly	1999-2024
Pitztaler-Gletscher	GSA	46.9270	10.87917	2863	hourly	1994-2024
Vent <sup>a</sup>	ACInn	46.8583	10.91250	1890	daily	1935-2016
		46.7989	10.91276	1908	1-min	2015-2024
Hochebenkar <sup>a</sup>	ACInn	46.8370	11.00822	2565	10-min	2012-2014
Station Hintereis <sup>a</sup>	ACInn	46.7989	10.76037	3031	1-min	2020-2023
Proviantdepot <sup>a</sup>	UIBK-GEOG	46.8595	10.82407	2737	10-min	2019-2023
Bella Vista <sup>a</sup>	UIBK-GEOG	46.7828	10.79138	2805	10-min	2015-2023
Latschbloder <sup>a</sup>	UIBK-GEOG	46.8011	10.80659	2919	10-min	2013-2023
Vernagtbach <sup>a</sup>	BADW	46.8566	10.82847	2640	10-min	2002-2012

<sup>a</sup> Located within the Tumpen-Ötztal catchment

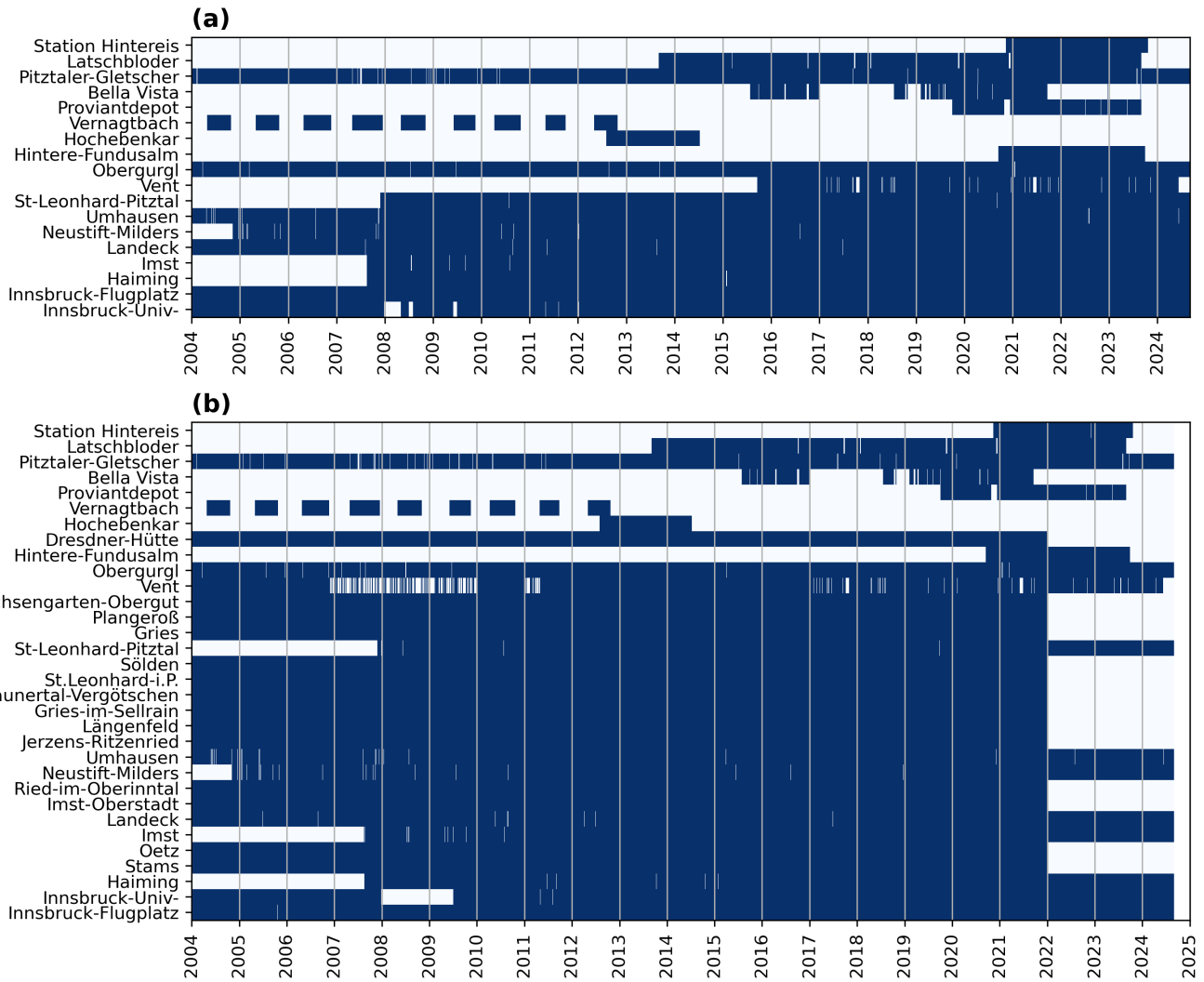


**Figure S2.** Overview of available (blue) and missing data (white) for weather station observed precipitation at hourly (a) and daily (b) resolution during the study period (2004-2024). Stations are sorted lowest (bottom) to highest (top) elevation.

### S1.3 IDF curves

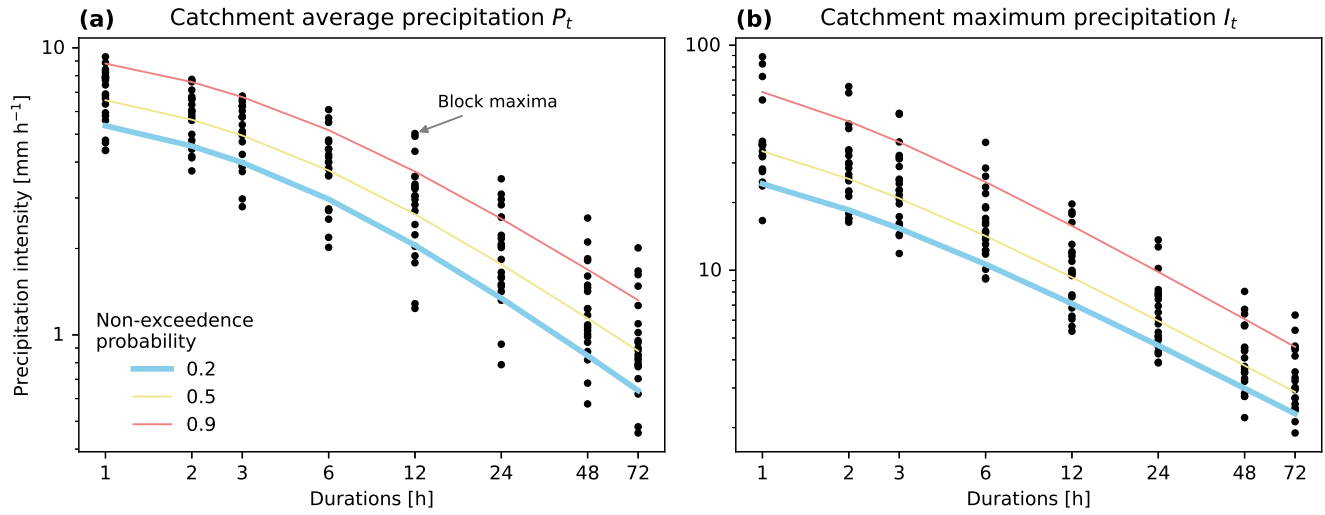


**Figure S3.** Intensity-duration-frequency (IDF) curves for catchment-averaged precipitation  $P_t$  and grid-scale maximum precipitation  $I_t$ . Black dots show annual May-October block maxima for each duration. The 0.2 non-exceedence probability (blue line) was the threshold used to detect heavy precipitation events in  $P_t$  and  $I_t$ .

## S2.1 INCA uncertainty

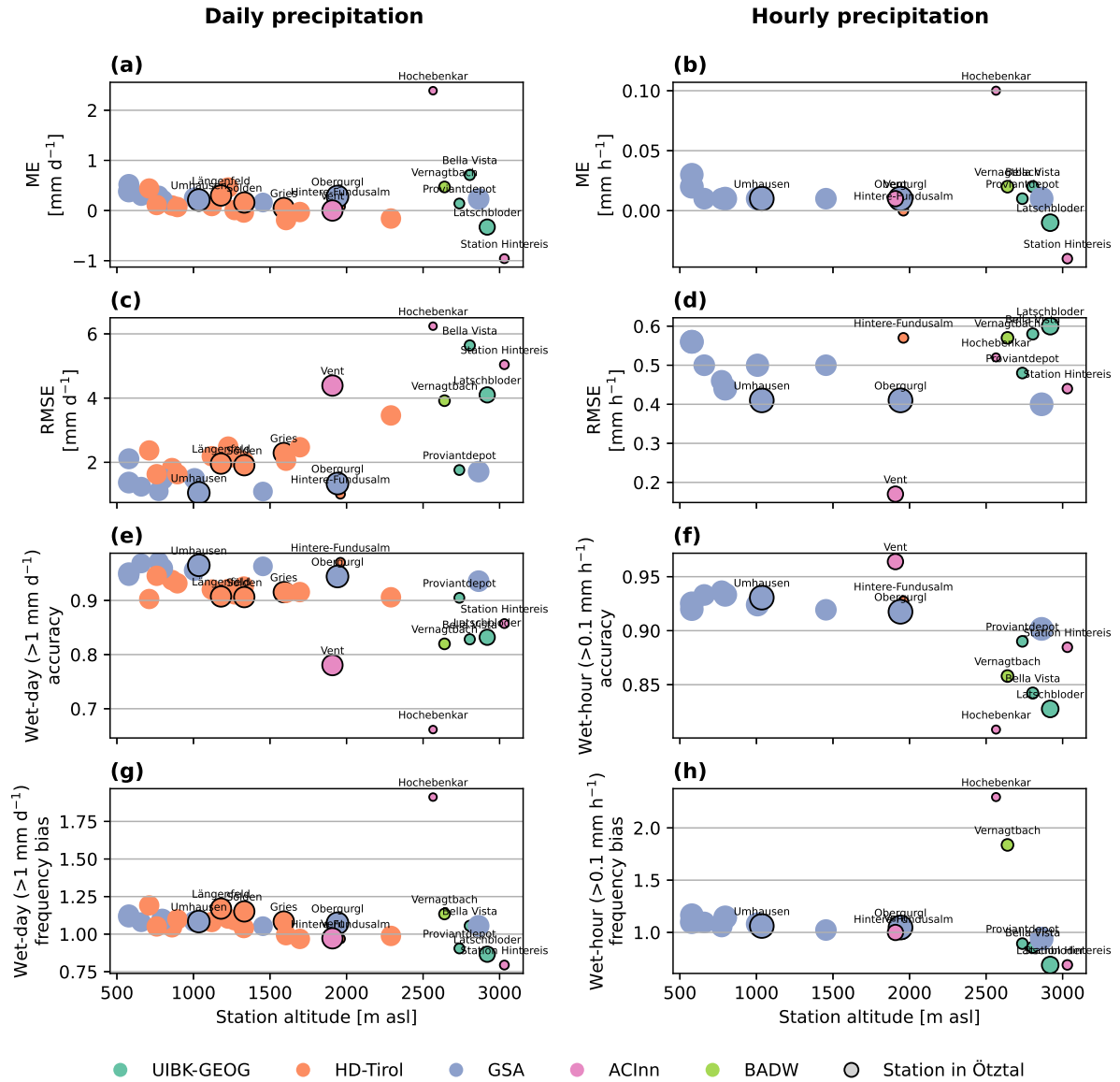


**Figure S4.** Uncertainty analysis of daily and hourly INCA precipitation when compared with weather station data. Each metric, the mean error (ME), root mean squared error (RMSE), precipitation occurrence accuracy (Acc), and precipitation occurrence frequency bias (FB) is plotted against the altitude of the station. Dot size is proportional to the number of time steps with valid INCA and station value pairs. Stations that are located within the study area of Ötztal are labelled.

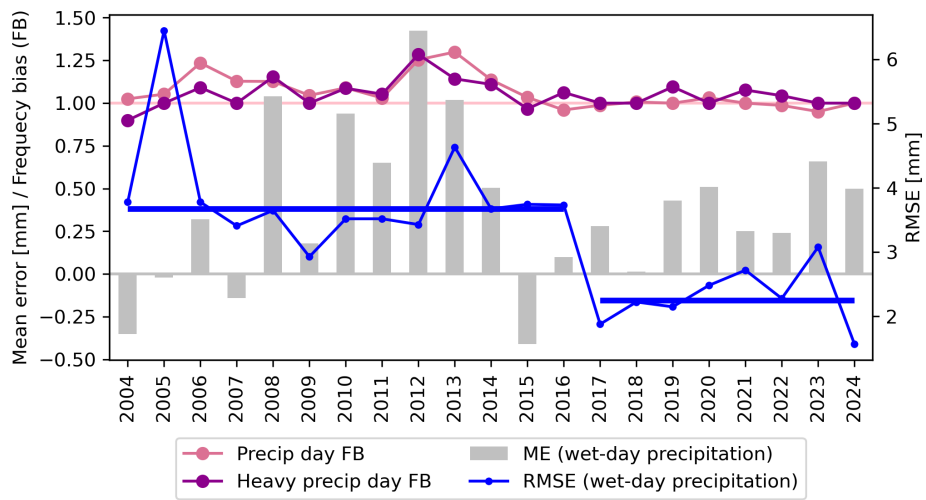


**Figure S5.** Uncertainty metrics for wet days only.

## S2.2 Heavy precipitation events and characteristics

### S2.2.1 Events removed due to unrealistic precipitation

Each of the three events removed due to an unrealistic precipitation pattern were detected from the grid-scale maximum precipitation time series  $I_t$ . For event 2019-d and 2017-l we found it suspicious that so much precipitation had occurred during the 3 and 12 hours of the events in only a few grid cells, while the rest of the catchment received no precipitation at all.

Given the location of the precipitation at the catchment boundary, it is conceivable that precipitation is mainly occurring on the other side of the watershed divide. It is still uncertain whether any precipitation actually fell within the Tumpen-Ötztal catchment, and at any rate, since the rest of the catchment had no precipitation, it is unlikely to be a heavy precipitation event.

In event 2017-k only a single grid cell received 300 mm of precipitation while the neighbouring cells received much less. This does not appear to be a realistic precipitation pattern. Furthermore, when scanning the INCA dataset for implausibly high precipitation values, that particular grid cell appeared often with very high precipitation rates. Hence, we assumed that event 2017-k was an event where some detection error in the radar caused it to appear to rain at high (but not implausibly high) rates for most of the 58 hours of the event.

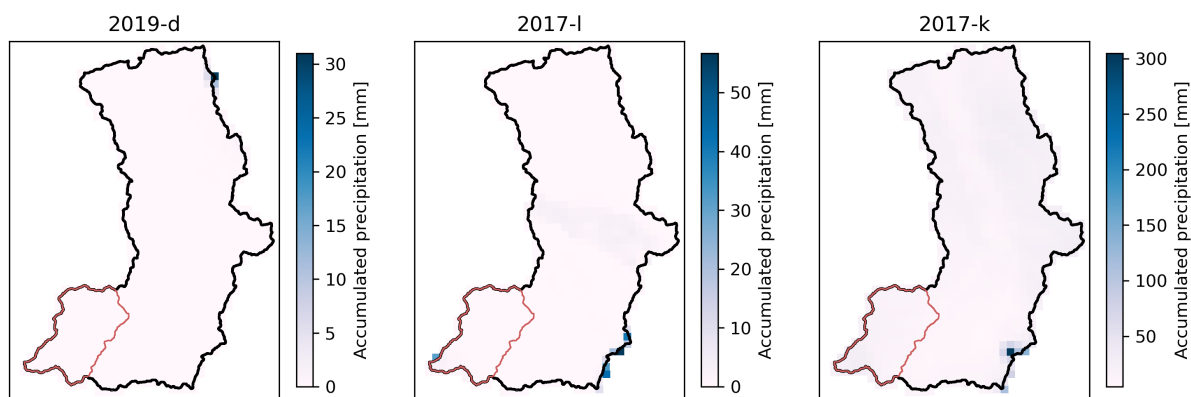


**Figure S6.** Maps of accumulated precipitation for the 3 events removed from the heavy precipitation catalogue.

### S2.2.2 Trend in numbers of heavy precipitation events

To assess whether the increasing trend in the number of extreme precipitation events detected from the INCA gridded product could be influenced by the data assimilation or calibration process, we analysed precipitation extremes at selected weather stations used in the development of INCA (Haiden et al., 2011). Using the same event-detection methodology as applied to the catchment-scale precipitation time series, we examined three Geosphere Austria stations: Obergurgl and Umhausen, located within the Tumpen-Ötztal catchment, and Pitztaler Gletscher, a nearby high-elevation station in an adjacent catchment. It should be noted that station data represent point-scale conditions and cannot capture the spatial extent of precipitation events; consequently, event counts at individual stations are not directly comparable to catchment-scale detections and may miss localized extremes occurring elsewhere in the catchment. Over the period 2004–2023, all three stations exhibit an positive trend in the annual number of detected extreme precipitation events. The trend is statistically significant at the Umhausen station (Mann–Kendall test, 5% significance level), while the trends at Obergurgl and Pitztaler Gletscher are positive but not significant. These results support the presence of a coherent increase in extreme precipitation frequency at the station scale and suggest that the trend observed in the INCA-based analysis is not solely an artifact of the gridded product.

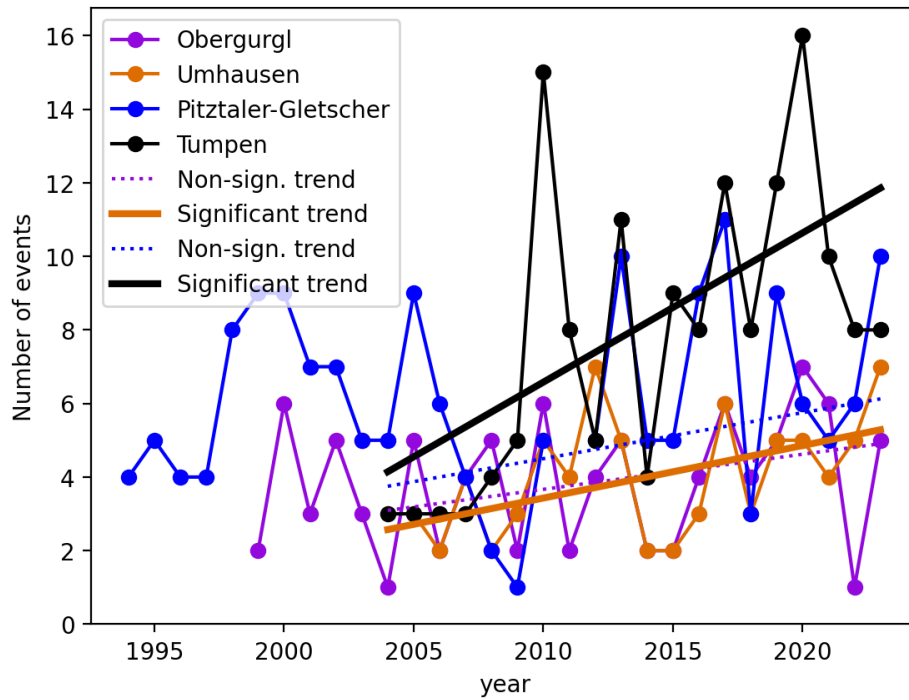


**Figure S7.** Heavy precipitation events detected at two stations within Tumpen-Ötztal, Umhausen and Obergurgl, in addition to a high-elevation station close to the Vent-Rofental catchment, Pitztaler Gletscher. The event numbers detected in the Tumpen-Ötztal catchment with the INCA dataset are shown in black. Trends in event numbers between 2004 and 2023, are shown.

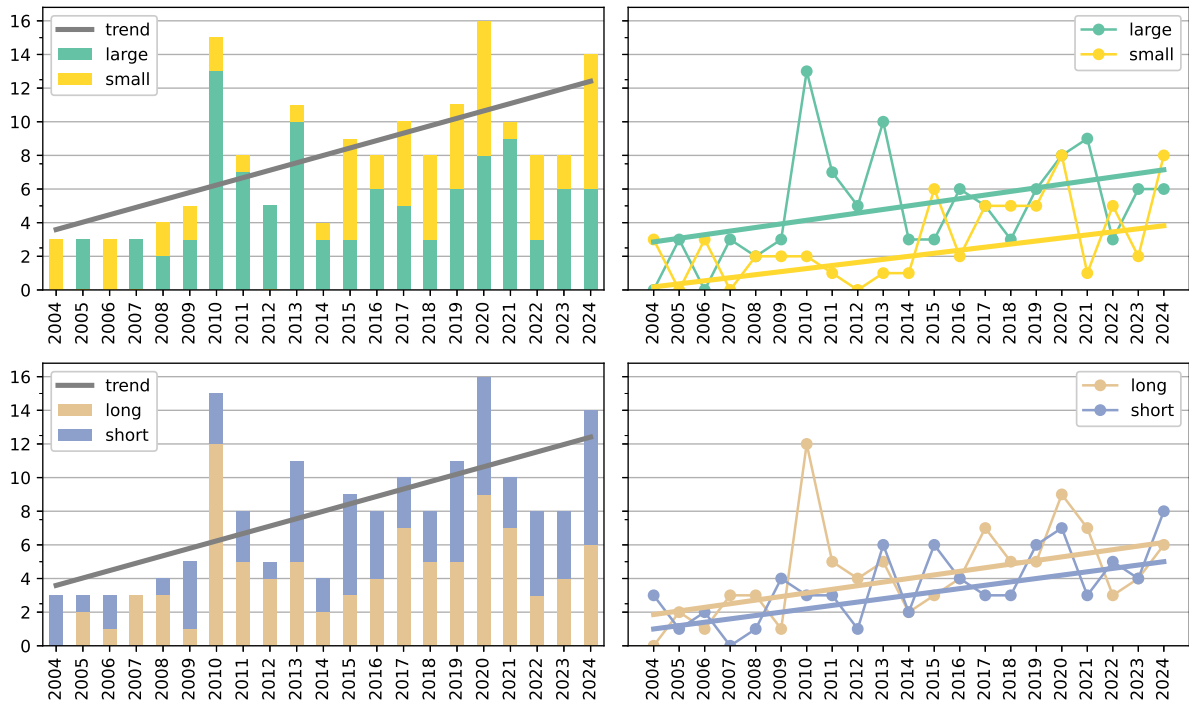


**Figure S8.** Trends in event numbers by spatial scale or temporal scale classification.

## S2.3 Precipitation characteristics and sediment response

**Table S2.** Heavy precipitation event numbers classified by temporal scale, spatial scale, or both.

	<b>Long-duration</b>	<b>Sub-daily</b>	All
<b>Catchment-wide</b>	73	31	104
<b>Localised</b>	18	44	62
All	91	75	<b>166</b>

### S2.3.1 Sediment response of heavy precipitation by spatial scale

#### 50 S2.4 Choice of linear regression model

Linear regression models were applied after  $\log_{10}$ -transforming the sediment response variables, which is typical for sediment transport processes. We evaluated the assumption of a linear relationship between the transformed sediment response variables and the heavy precipitation event characteristics by examining the residuals from all regression models. Since the residuals were approximately normally distributed (Fig. S10), we therefore consider linear regression to be an appropriate and robust first-order approach for characterizing the relationships between precipitation characteristics and sediment response, while acknowledging that non-linear behaviour may exist at finer scales or under specific conditions.

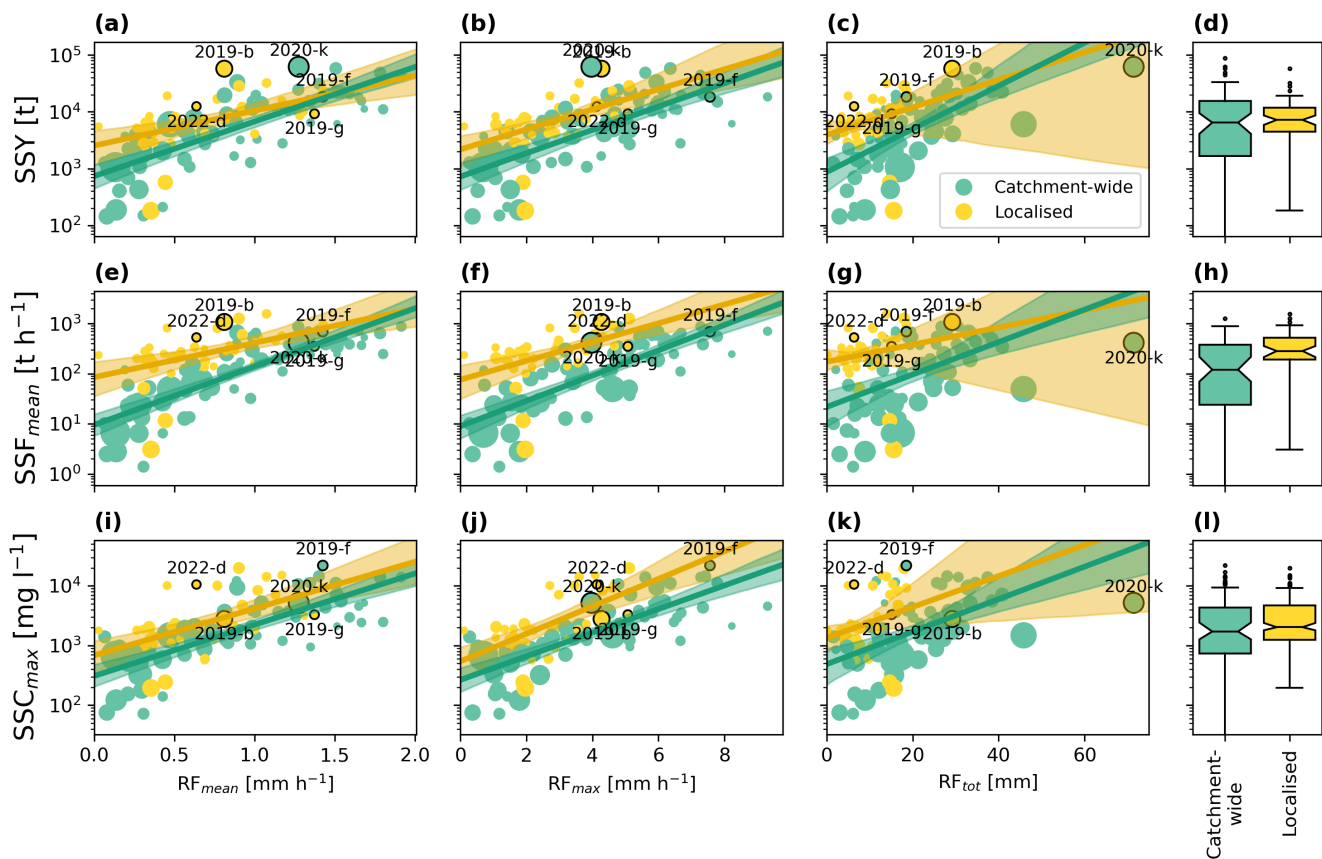


**Figure S9.** Suspended sediment response to heavy precipitation events (107 events between 2011 and 2022) in terms of their mean intensity of catchment-averaged rainfall  $RF_{mean}$  (a,e,i), maximum intensity of catchment-averaged rainfall  $RF_{max}$  (b,f,j), and total cumulative catchment-averaged rainfall  $RF_{tot}$  (c,g,k). There are 67 catchment-wide and 40 localised heavy precipitation events. The increase in sediment response variables with rainfall intensity and totals is similar for both localised (grid scale) and catchment-wide heavy precipitation events. Lines are means from linear regression, and shaded areas are 95% bootstrap confidence intervals based on 1000 randomisations. Labelled events are the same as in Fig. 4. See Fig. 6 for details on boxplot configuration.

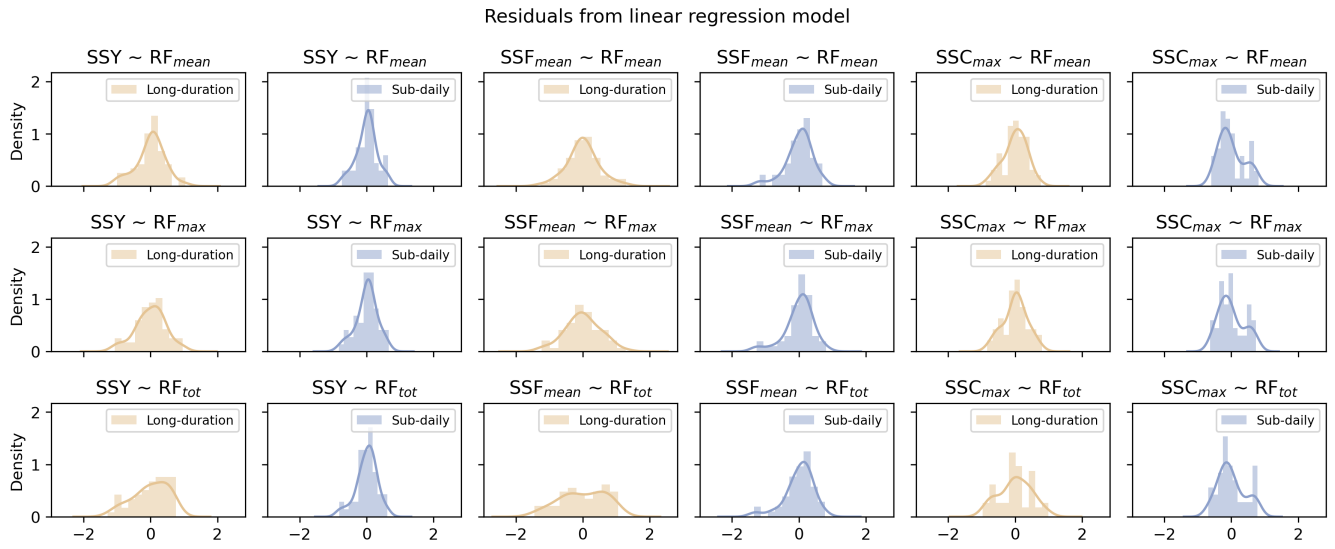


**Figure S10.** Residuals from linear regression model of sediment response to different heavy precipitation event characteristics, classified by temporal scale.

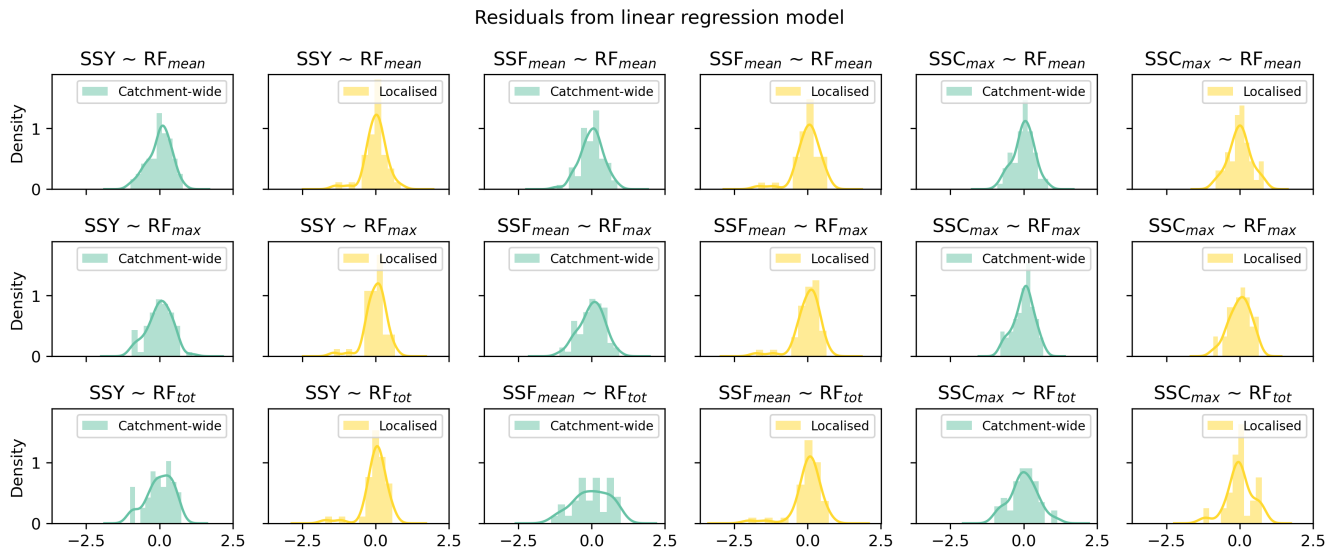


**Figure S11.** Residuals from linear regression model of sediment response to different heavy precipitation event characteristics, classified by spatial scale.

## S2.4.1 Distribution of bootstrapped slopes

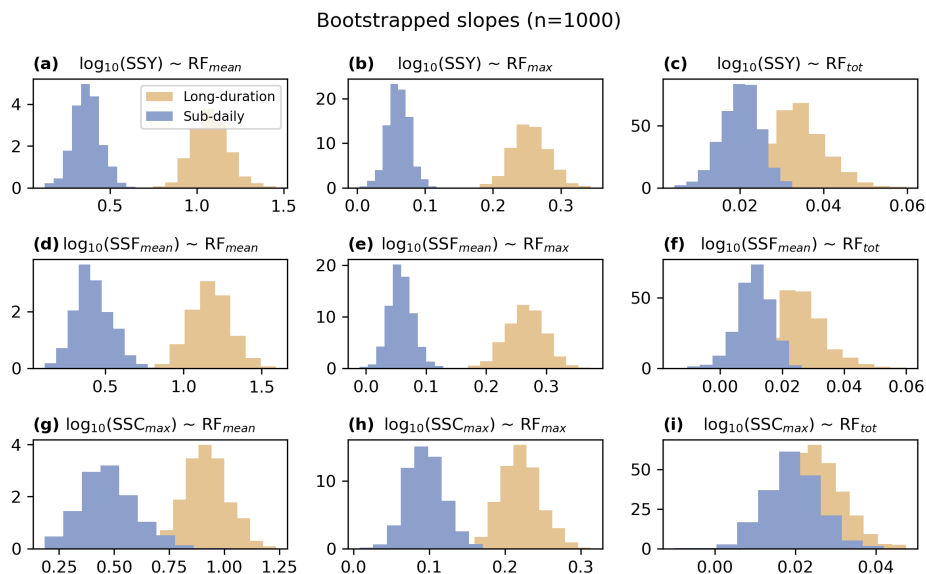


**Figure S12.** Histograms of the 1000 bootstrapped slopes from the linear regression models fitted to long-duration and sub-daily heavy precipitation events.

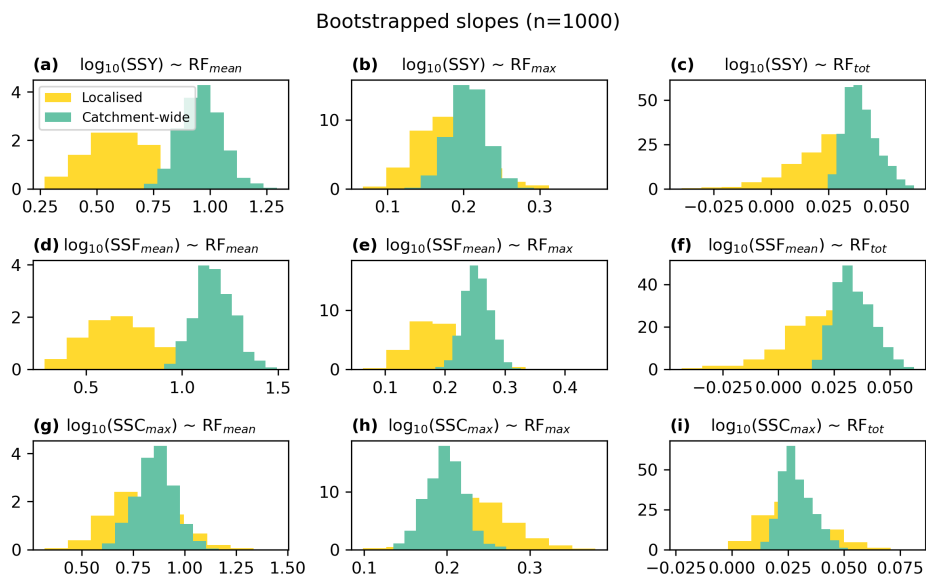


**Figure S13.** Histograms of the 1000 bootstrapped slopes from the linear regression models fitted to catchment-wide and localised heavy precipitation events.

## S2.5 All event metrics by temporal scale

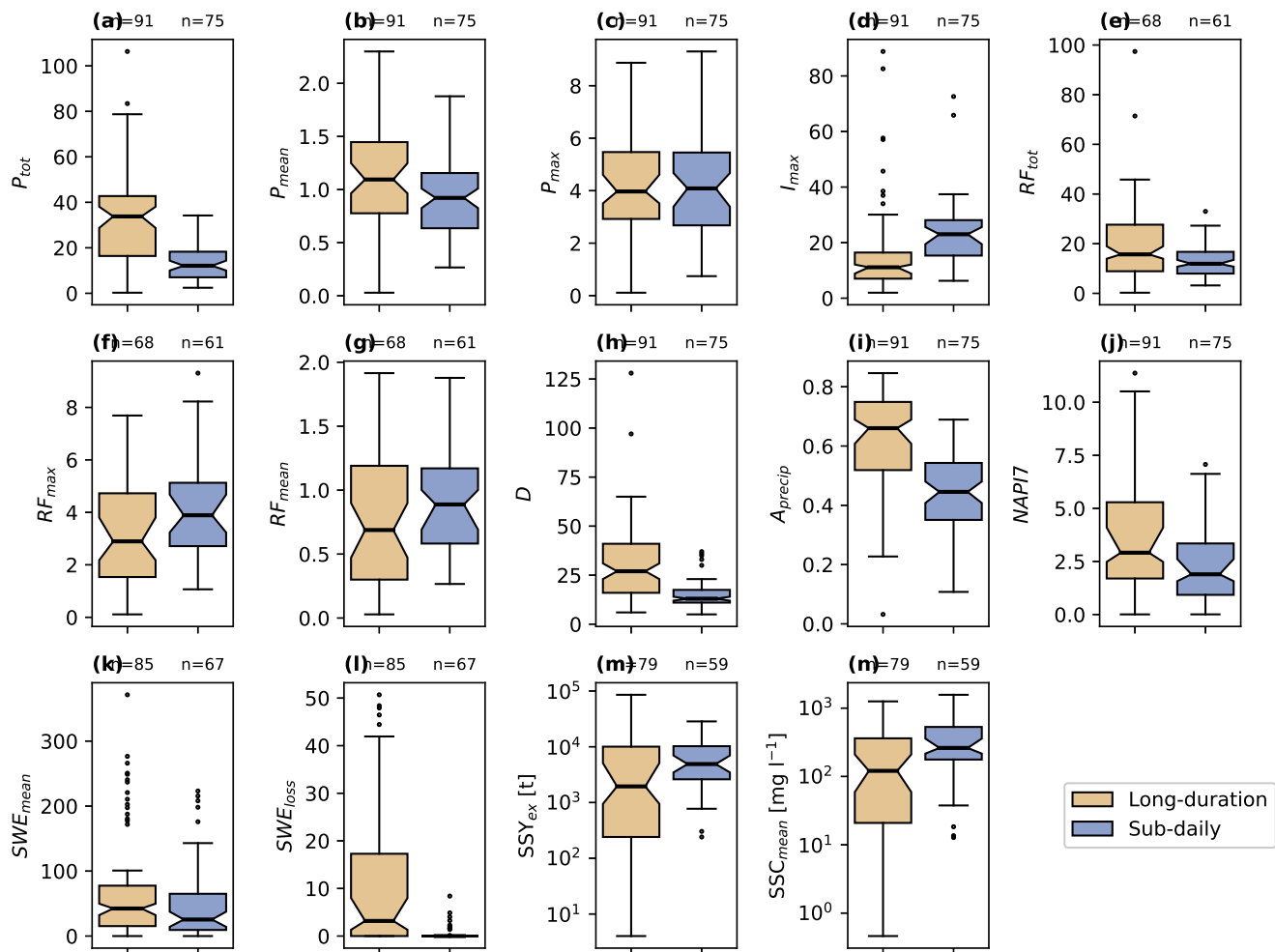


**Figure S14.** Boxplots with all precipitation characteristics and sediment response variables not already show in the main manuscript, classified by temporal scale of heavy precipitation events.

## References

- 60 Copernicus Land Monitoring Service: CORINE Land Cover 2018 (raster 100 m) [data set], <https://doi.org/10.2909/960998c1-1870-4e82-8051-6485205ebbac>, 2020.
- Haiden, T., Kann, A., Wittmann, C., Pistotnik, G., Bica, B., and Gruber, C.: The Integrated Nowcasting through Comprehensive Analysis (INCA) System and Its Validation over the Eastern Alpine Region, *Weather and Forecasting*, 26, 166–183, <https://doi.org/10.1175/2010WAF2222451.1>, 2011.